0026-895X/08/7404-1072–1083$20.00
MOLECULAR PHARMACOLOGY
Copyright © 2008 The American Society for Pharmacology and Experimental Therapeutics
Mol Pharmacol 74:1072–1083, 2008

Vol. 74, No. 4
48405/3382043
Printed in U.S.A.

Patupilone-Induced Apoptosis Is Mediated by Mitochondrial Reactive Oxygen Species through Bim Relocalization to Mitochondria

N. R. Khawaja, M. Carré, H. Kovacic, M. A. Estève, and D. Braguer

Institut National de la Santé et de la Recherche Médicale Unité Mixte de Recherche 911, Centre de Recherche en Oncologie Biologique et Oncopharmacologie; Université Aix-Marseille, Marseille, France

Received April 30, 2008; accepted July 1, 2008

ABSTRACT

Among the new microtubule-targeted agents, the epothilone family of molecules has shown promising anticancer potential, and clinical trials are currently underway for patupilone (epothilone B) in various cancer indications. In this study, we characterized novel aspects of patupilone's cellular action that may underlie its potent cytotoxicity in human neuroblastoma cells. Patupilone induced mitochondrial membrane potential collapse, mitochondrial morphological changes, and cytochrome *c* release, leading to apoptosis. Within the first 2 h, patupilone increased the generation of reactive oxygen species (ROS; i.e., superoxides and hydrogen peroxide, 33 ± 6 and 51 ± 3% increase, respectively), specifically from mitochondria. ROS scavengers and mitochondrial DNA depletion [$\rho^{(-)}$ cells] significantly protected cells against patupilone cytotoxicity, indicating that ROS generation is a key event in the initial phase of apoptosis. Although the Bim expression level was not modified by patupilone, this proapoptotic protein accumulated in the mitochondrial compartment (2.4-fold increase at IC_{70}) after only a 6-h treatment. In contrast, Bax and Bcl-2 mitochondrial levels were not changed during treatment. It is noteworthy that ROS inhibition prevented Bim relocalization to mitochondria and mitochondrial membrane changes induced by patupilone. Altogether, our data reveal that patupilone-mediated ROS production by mitochondria initiates the intrinsic signaling cascade by inducing Bim accumulation in mitochondria. These results might explain the superior activity of patupilone in tumor cells compared with paclitaxel that is, until now, the clinical reference among microtubule-stabilizing agents. Furthermore, our data highlight the importance of mitochondria that simultaneously assume the role of activator and integrator of apoptotic signals triggered by patupilone.

Microtubules play a basic role in diverse cellular functions, including cell division and trafficking of intracellular organelles, vesicles, and proteins. They are very dynamic structures and are referred as successful targets for microtubule-targeted agents (MTAs) in cancer chemotherapy (Jordan and Kamath, 2007). MTAs suppress microtubule dynamics in tumor cells, which generally results in impairment of both mitotic and interphasic networks (Pasquier et al., 2006). These drugs are also potent inducers of apoptosis, a complex programmed cell-death process that involves intrinsic signaling cascades converging to mitochondria (Pourroy et al., 2004).

Among MTAs, taxanes are microtubule-stabilizing agents, which are widely used in cancer therapy. Despite their demonstrated effectiveness, their clinical success has been severely hindered by the emergence of resistant tumor cells. Acquired resistance can result from the enhanced expression of P-glycoprotein (P-gp), tubulin mutations or changes in microtubule subtypes composition, and alterations in apoptotic signaling pathways (Ferlini et al., 2003; Orr et al., 2003; Sève et al., 2007). These limitations have led to an intensive search for new microtubule-stabilizing agents, which resulted in isolation of the epothilone family of molecules from myxobacterium *Sorangium cellulosum*. Among them, patupilone (epothilone B, EPO906) has shown a promising anticancer activity in vitro and in vivo and is currently undergoing phase III clinical trials. It is interesting that epothilones are active against P-gp-overexpressing cancer cells resistant to paclitaxel (Taxol) (Altmann et al., 2007). Elsewhere, although epothilones bind to the same β-tubulin site as tax-

This work was partly supported by the Cancéropole PACA and INCa (France), and N.R.K. received a fellowship from the Higher Education Commission of Islamabad, Pakistan.

Article, publication date, and citation information can be found at http://molpharm.aspetjournals.org.

doi:10.1124/mol.108.048405.

ABBREVIATIONS: MTA, microtubule-targeted agent; P-gp, P-glycoprotein; MTT, 3-(4,5-dimethylthiazol-2-yl)-2,5-diphenyltetrazolium bromide; DMSO, dimethyl sulfoxide; DCF-DA, dichlorofluorescein diacetate; ROS, reactive oxygen species; COX II, cytochrome *c* oxidase II; WST-1, 2-(4-iodophenyl)-3-(4-nitrophenyl)-5-(2, 4-disulfophenyl)-2H; KCN, potassium cyanide; JNK, c-Jun NH_2-terminal kinase.

anes (Bollag et al., 1995; Nettles et al., 2004), they remain active against cells and xenograft models that have developed resistance to taxanes as a result of tubulin subtype mutations or overexpression (Nicolaou et al., 1997; Lee et al., 2008). In addition, the microtubule-stabilizing activity of epothilones is not always related to their antitumor effectiveness (Nicolaou et al., 1997). Thus, other cellular targets and specific mechanisms of action may exist for this new class of MTAs.

Mitochondria are essential cellular organelles for ATP synthesis, reactive oxygen species (ROS) homeostasis, and apoptosis orchestration (Newmeyer and Ferguson-Miller, 2003). Their central role in apoptosis induction by MTAs is now uncontested (Estève et al., 2007). Disruption of the mitochondrial membrane potential and release of death-promoting factors like cytochrome *c* are critical proapoptotic events, which are largely reported to be controlled by the Bcl-2 family of proteins (Adams and Cory, 2007). The relative levels of pro- and antiapoptotic members of the Bcl-2 family, localized in the mitochondrial compartment, determine the cell susceptibility to apoptosis. It is interesting that variations in cell sensitivity to paclitaxel have been related to Bim expression levels (Putcha et al., 2001; Li et al., 2005, 2007). Without apoptotic stimulus, Bim may be sequestered in the microtubule cytoskeleton through its binding to dynein motor complexes (Puthalakath et al., 1999). However, no evidence exists regarding Bim relocalization during apoptosis induced by microtubule-stabilizing agents.

Mitochondrial respiratory chain complexes are key sources of ROS, well known mediators of various biological responses (Archer et al., 2008). It has been shown that paclitaxel enhanced ROS production from both mitochondria and NADPH oxidase (Varbiro et al., 2001; André et al., 2002; Alexandre et al., 2006). Moreover, antioxidants protected cells against apoptosis induced by docetaxel, indicating that ROS accumulation could contribute to the cell death process induced by microtubule-stabilizing agents (Taniguchi et al., 2005). However, the early apoptotic route induced by MTA-mediated mitochondrial ROS generation in cancer cells has not yet been explored.

In this study, we show that early ROS production from mitochondria plays an important role in the onset of patupilone-induced apoptosis through modifications in mitochondrial membrane permeability. Indeed, this is the first study showing that ROS generated by mitochondria mediates, in turn, Bim relocalization to mitochondria. We thus characterized novel aspects of patupilone's cellular action that may underlie its potent growth inhibition of human tumor cells.

Materials and Methods

Drugs and reagents. Patupilone (epothilone B) and epothilone A were kindly provided by Dr. M. Wartmann (Novartis Pharma AG, Basel, Switzerland) as pure substances and were dissolved in DMSO to obtain stock solutions. Stock solutions of 2-(4-iodophenyl)-3-(4-nitrophenyl)-5-(2, 4-disulfophenyl)-2H (WST-1) (Interchim, Montluçon, France), DCF-DA (Molecular Probes, Eugene, OR), lucigenin, NADPH, allopurinol, and rotenone (Sigma, St. Louis, MO) were dissolved in DMSO. Potassium cyanide (KCN), 4, 5-dihydroxybenzene-1, 3-disulfonic acid disodium salt (tiron) (Sigma) were prepared in sterile water, and sodium pyruvate was purchased from Invitrogen (Carlsbad, CA).

Cell Culture and Drug Treatment. Human neuroblastoma SK-N-SH and IMR-32 cells were routinely maintained in culture medium according to standard procedures (André et al., 2000; Pourroy et al., 2004). Cells (37×10^3 cells/cm^2) were seeded 72 h before treatment. For coincubation experiments, tiron was added at 2 mM, sodium pyruvate at 10 mM, allopurinol (3,5,7,8-tetrazabicyclo[4.3.0] nona-3,5,9-trien-2) at 500 μM, rotenone [1,2,12,12a-tetrahydro-8,9-dimethoxy-2-(1-methylethenyl-(1)benzopyrano (2,4-*b*) furo (2,3-h)(1) benzopyran-6 (6H)] at 100 nM, and KCN at 100 μM. Rho-negative [$\rho^{(-)}$ SK-N-SH] cells were obtained by incubating SK-N-SH cells for 8 weeks with routine culture medium supplemented with 100 ng/ml ethidium bromide (2,7-diamino-9-phenyl-10-ethyl phenenthridinium bromide) sodium pyruvate (1 mM), uridine (50 μg/ml), and glucose (4.7 mg/ml) (Patenaude et al., 2007). These cells were then maintained in the same culture medium without ethidium bromide.

Cytotoxicity Assay. Growth inhibition of neuroblastoma cells and $\rho^{(-)}$ was studied after a 72-h treatment with drugs by using the MTT cell proliferation assay (Pourroy et al., 2004; Estève et al., 2006). For short-exposure treatments, after specific treatment duration (6 or 24 h), culture medium with drug was replaced with normal culture medium, and MTT assay was performed 72 h after treatment. Although comparing the impact of patupilone on $\rho^{(+)}$ and $\rho^{(-)}$ SK-N-SH, the seeding and treatment schedule of respective cells was designed in a manner that cell confluence was identical during treatment. P-gp was completely inhibited by 10 μM verapamil, as we

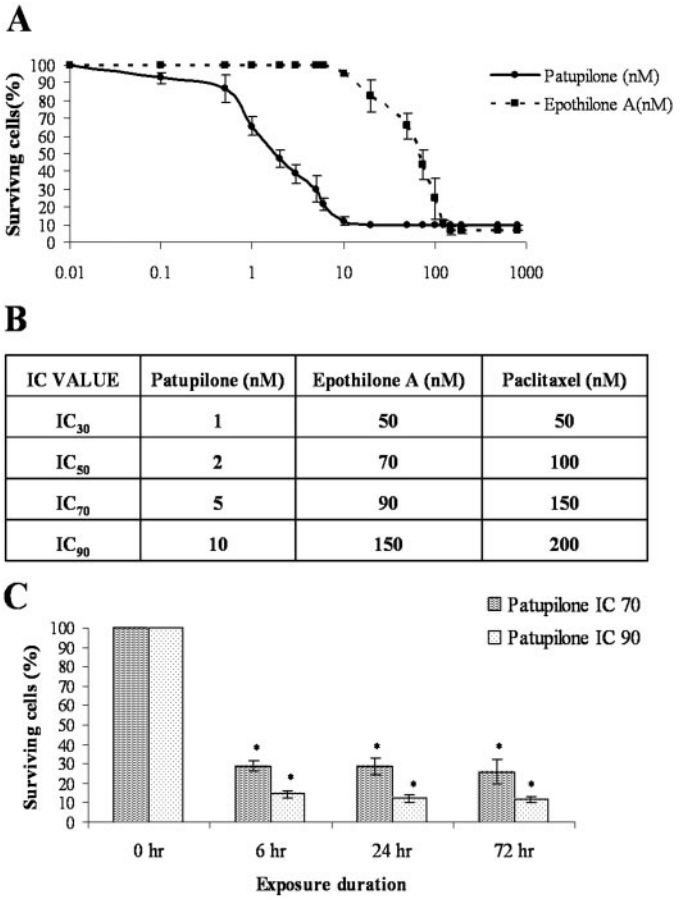

IC VALUE	Patupilone (nM)	Epothilone A (nM)	Paclitaxel (nM)
IC_{30}	1	50	50
IC_{50}	2	70	100
IC_{70}	5	90	150
IC_{90}	10	150	200

Fig. 1. Patupilone potently inhibits cell growth of human neuroblastoma SK-N-SH cells. A, concentration-dependent inhibition of cell survival by patupilone (epothilone B) and epothilone A after a 72-h treatment. B, table showing IC values for both epothilones and paclitaxel in SK-N-SH cells. C, SK-N-SH cells were treated with indicated patupilone concentrations for 6, 24, and 72 h. After short-term treatment (6 or 24 h), culture medium with drug was replaced with normal culture medium. MTT assay was performed 72 h after treatment in either condition (*, $p < 0.05$ versus control). Results represent means ± S.D.

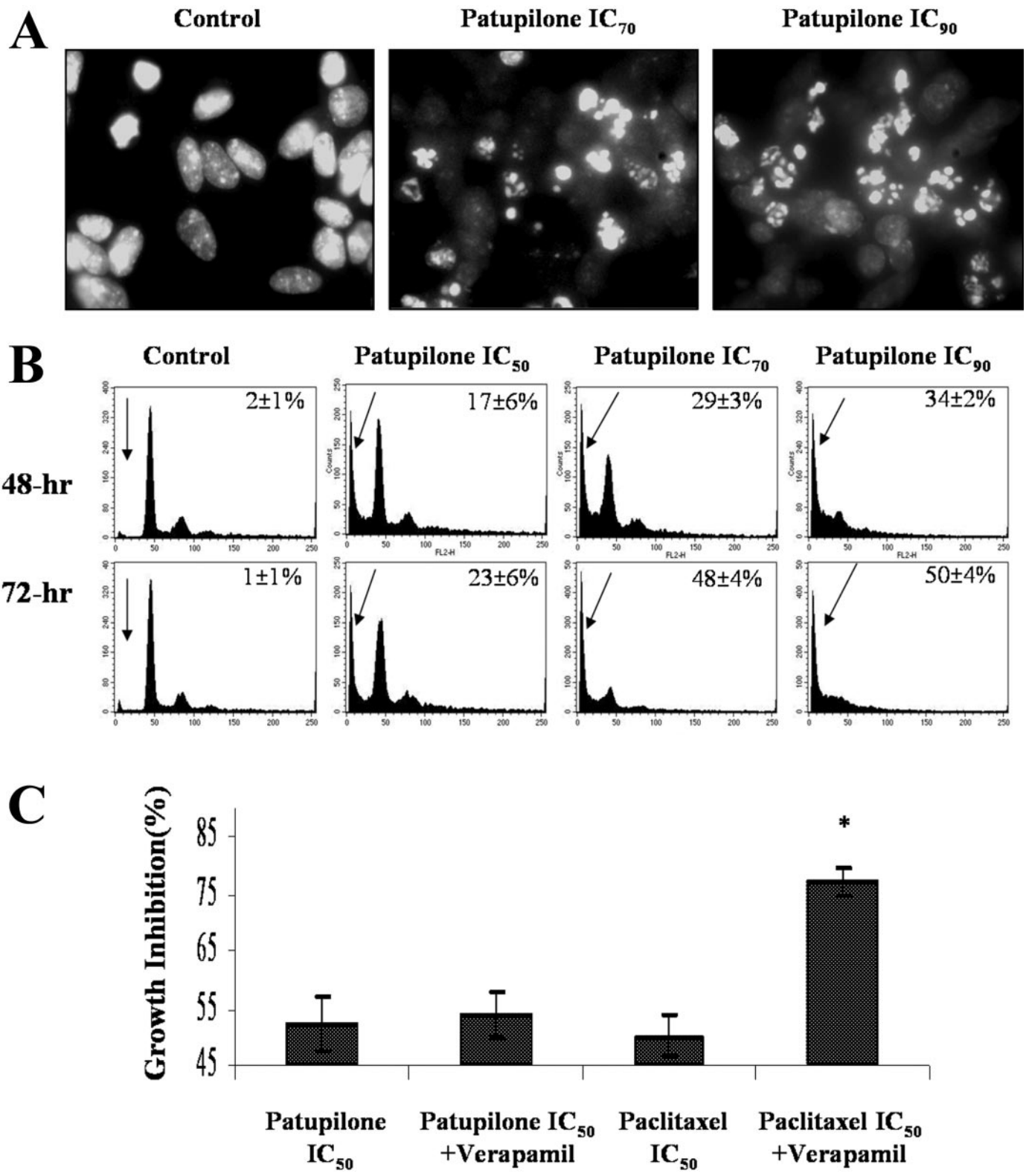

Fig. 2. Patupilone induces apoptosis, regardless of multidrug resistance status. A, fluorescence analysis of nuclei fragmentation after a 48-h treatment of SK-N-SH cells with patupilone IC_{70} (40× objective). Results are representative of three independent experiments. B, SK-N-SH cell cycle analysis by flow cytometry. The sub-G_1 population is indicated by an arrow, and the corresponding percentage is indicated. C, sensitivity of SK-N-SH cells to patupilone and paclitaxel at their respective IC_{50} values (2 and 100 nM) in the presence or absence of verapamil 10 μM. Data are expressed as mean ± S.D. *, $p < 0.05$ versus control.

determined previously (Estève et al., 2006). At least three independent experiments (in quadruplicate) were performed for each respective condition.

Flow Cytometry. SK-N-SH cells were fixed, permeabilized, and stained with propidium iodide as described previously (Pourroy et al., 2004; Estève et al., 2006). Measurement of fluorescence was performed by flow cytometry (FACScan; BD Biosciences, San Jose, CA). Results obtained were analyzed by CellQuest Pro software (BD Biosciences). At least three independent experiments were performed for each condition.

Fluorescent Microscopy. Cells were grown on eight-well plates and incubated with drugs for 48 h. Cells were then fixed with 3.7% formaldehyde, permeabilized with 1% saponine, and successively incubated with the anti-cytochrome *c* antibody (BD Biosciences Pharmingen, San Diego, CA) and a secondary antibody conjugated with fluorescein isothiocyanate (Jackson ImmunoResearch Laboratories, West Grove, PA) as described previously (Pourroy et al., 2004; Estève et al., 2006). For nuclei visualization, cells were additionally stained with 4′,6-diamidino-2-phenylindole. Cells were observed using a Leica DM-IRBE microscope coupled with a digital camera (charge-coupled device camera Cool SnapFX; Princeton Instruments, Monmouth Junction, NJ), and results were analyzed with Metamorph software (Universal Imaging Corporation, Downingtown, PA).

Mitochondria Isolation and Western Blotting. Mitochondria were isolated from treated SK-N-SH cells as we described previously (André et al., 2000). Equal amounts of proteins from mitochondrial pellets or whole cells were separated by SDS-polyacrylamide gel electrophoresis and electrotransferred onto a nitrocellulose membrane. Primary antibodies used were directed against p53 and cytochrome *c* oxidase II (COX II; Santa Cruz Biotechnology, Santa Cruz, CA); p21/WAF1 (Oncogene Research Product, San Diego, CA); Bim, Bak, and Bax (Santa Cruz Biotechnology); Bcl-2 (Dako Denmark A/S, Glostrup, Denmark); cytochrome *c* (BD Biosciences Pharmingen); voltage-dependent anion channel, and α-tubulin (Sigma). Peroxidase-conjugated goat anti-mouse, donkey anti-rabbit antibodies (Jackson ImmunoResearch Laboratories) and donkey anti-goat (Santa Cruz Biotechnology) were used as secondary antibodies. Visualization was accomplished using an enhanced chemiluminescence detection kit (GE Healthcare, Chalfont St. Giles, Buckinghamshire, UK). Protein quantification of blots was performed by using ImageJ software (http://rsbweb.nih.gov/ij/). Three independent experiments were performed.

Electron Microscopy. After treatment with patupilone IC_{70} and/or tiron, cells were fixed with 2.5% glutaraldehyde for 10 min. Then cells were scratched mechanically, dehydrated in ethanol, embedded in Epon, and cut into thin sections as described previously (André et al., 2002). The samples were imaged by a transmission electron microscope (JEOL 1220; Jeol, Croissy sur Seine, France). At least 200 mitochondria were analyzed in three independent experiments (IPS Samba Technologies, Grenoble, France).

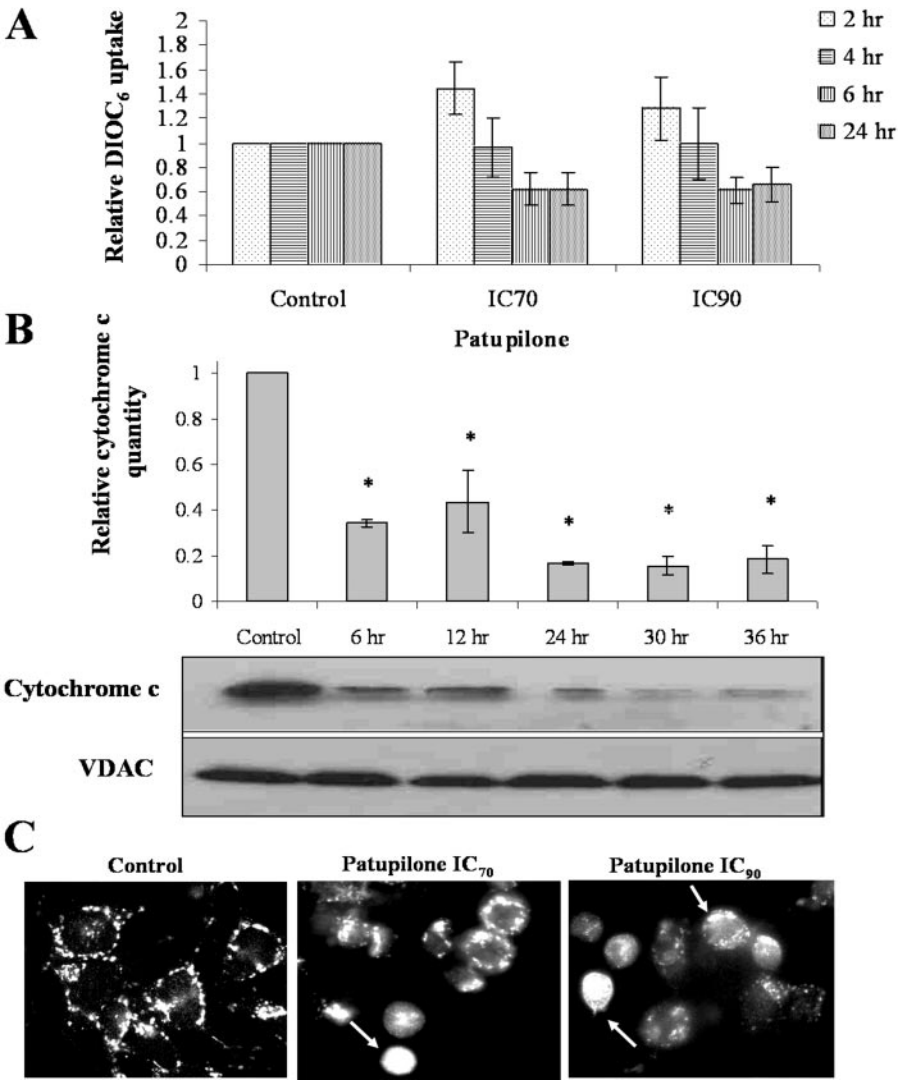

Fig. 3. Patupilone induces changes in mitochondrial membrane permeability. A, measurement of the mitochondrial membrane potential collapse by 3,3′-dihexyloxacarbocyanine iodide incorporation in human neuroblastoma SK-N-SH cells. B, Western blot analysis of cytochrome *c* contained in mitochondria isolated from SK-N-SH cells treated with patupilone IC_{70} (up to 36 h). C, immunofluorescence analysis of cytochrome c after a 24-h treatment with patupilone. Arrows show typical cells with released cytochrome *c*. Blots, pictures, and cytograms are representative of at least three independent experiments. Results were expressed as mean ± S.D., and significant differences were determined compared with vehicle-treated cells (*, $p < 0.05$).

Measurement of Reactive Oxygen Species. Superoxide ions generation was measured by either WST-1 colorimetric test or lucigenin chemiluminescence. Cells were treated, in 96-well plates with patupilone and ROS scavengers/inhibitors before incubation with WST-1 (500 μM) for 30 min. For the chemiluminescence test, cells were suspended in a solution containing lucigenin (0.3 mg/ml) and NADPH (17 mg/ml) during 2-h treatment (Morazzani et al., 2004). Hydrogen peroxide production was evaluated by H2-DCF-DA fluorescence as described previously (Morazzani et al., 2004). Concentration of H2-DCF-DA used was extended to 100 μM in our conditions. Lucigenin and H2-DCF-DA ROS measurements were both performed using a Fluoroskan Ascent FL plate reader (Thermo Fisher Scientific, Courtaboeuf, France), and WST-1 measurements with Labsystems Multiscan RC (Honoré et al., 2003). All measurements were performed at 37°C.

Statistical Analysis. Results are expressed as means ± S.D. from at least three independent experiments. Statistical analysis was done using Student's t test. The value of $p < 0.05$ was considered statistically significant.

Results

Patupilone Potently Induces Apoptosis in Human Neuroblastoma Cells, Regardless of the Multidrug Resistance Status. We first determined that patupilone inhibited SK-N-SH cell growth at low nanomolar concentrations (Fig. 1, A and B). After a 72-h treatment, the IC_{50} value was only 1.9 nM. Epothilone A was considerably less active than patupilone because its IC_{50} value reached 70 nM. Patupilone was also 50 times more potent in SK-N-SH cells than paclitaxel (IC_{50} = 100 nM), which is the clinical reference compound among microtubule-stabilizing agents (Fig. 1, A and B). It is interesting that 6- as well as 24-h exposure of cells with patupilone induced the same level of cytotoxicity as 72 h of drug exposure ($p > 0.05$, Fig. 1C), indicating that early patupilone effects were sufficient for its activity. During patupilone treatment, a marked fraction of the population of cells displayed apoptotic characteristics (nuclei fragmentation and sub-G_1 cells) (Fig. 2, A and B).

In contrast to the taxanes and other MTAs, patupilone has been reported not to be subject to P-gp-mediated drug efflux. Here, we found that patupilone was as active in the P-gp-overexpressing cells SK-N-SH (IC_{50} = 1.9 ± 0.3 nM) as in the P-gp-negative ones, IMR-32 cells (IC_{50} = 1.4 ± 0.5 nM, $p > 0.05$) (data not shown). Inhibition of P-gp by verapamil did not modify patupilone cytotoxicity in SK-N-SH cells, confirming that patupilone is not a substrate of P-gp (Fig. 2C). In sharp contrast, P-gp inhibition increased paclitaxel cytotoxicity in SK-N-SH cells (100 nM became IC_{80}) but it remained insufficient to render it as potent as patupilone (IC_{80} = 5.5 nM) (Fig. 2C). Finally, paclitaxel was also significantly less

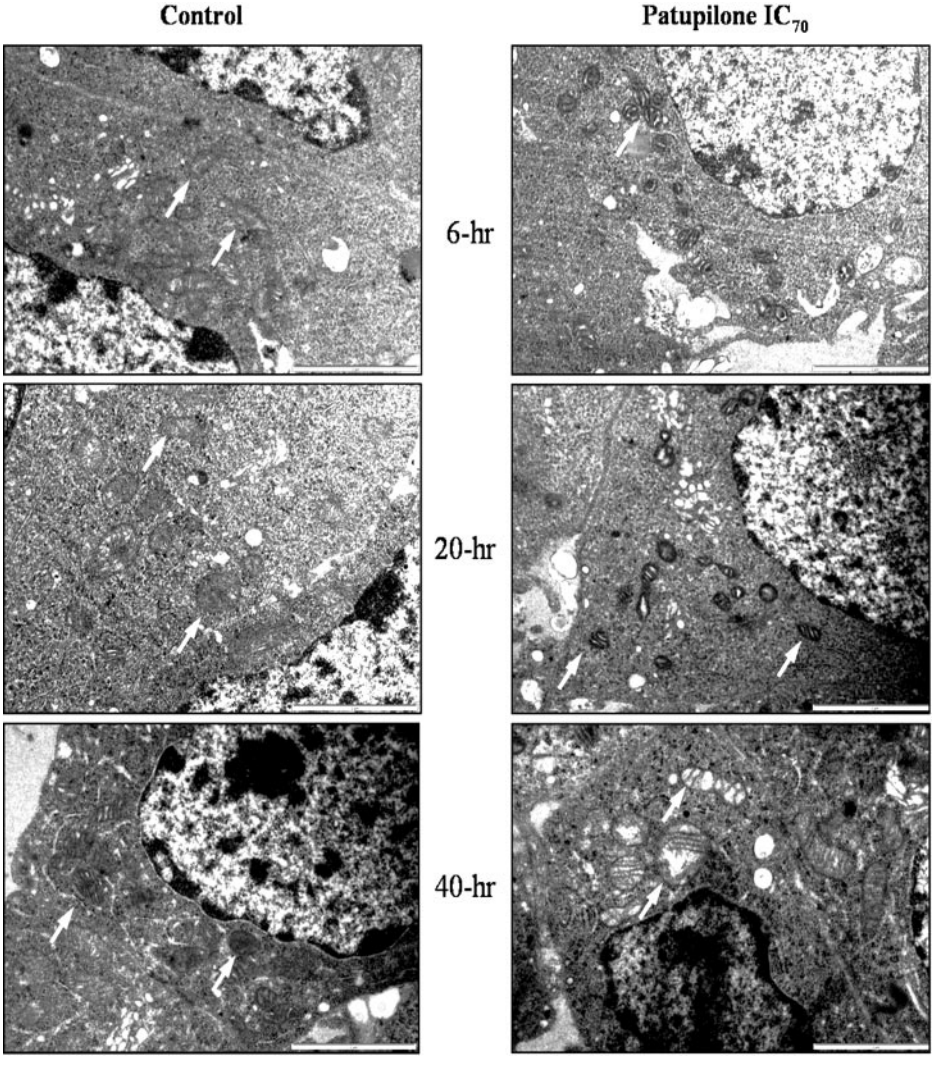

Fig. 4. Patupilone induces changes in mitochondria morphology. Visualization, by transmission electron microscopy, of mitochondria morphology in SK-N-SH cells treated with vehicle (control) or patupilone IC_{70}. Arrows show typical control mitochondria in the left column, and both "striped" (6–20 h) and swelled mitochondria (40 h) in the right column. Bar, 2 μm.

active than patupilone in P-gp-negative IMR-32 cells (IC_{50} = 6.3 ± 0.3 and 1.4 ± 0.5 nM, respectively, $p < 0.01$). Thus, the difference in cell sensitivity to these MTAs was probably due not only to the P-gp status of neuroblastoma cells but also to patupilone's enhanced ability to activate apoptotic signals.

Patupilone Alters Mitochondria Function and Morphology. To determine whether patupilone activates the intrinsic apoptosis pathway, we first measured the mitochondrial membrane potential variations from 2- to 24-h treatment (Fig. 3A). At 6 h of treatment with IC_{70} of patupilone, mitochondrial membrane depolarization was observed (38 ± 4% decrease in 3,3′-dihexyloxacarbocyanine iodide uptake; $p < 0.05$). After a 24-h treatment, the membrane potential collapse was not amplified ($p > 0.05$ compared with 6 h), indicating that patupilone induced maximal changes in mitochondrial membrane integrity as soon as 6 h of treatment. We then studied whether mitochondrial membrane depolarization was associated with the release of proapoptotic factors from the intermembrane space. Therefore, we isolated mitochondria from control and patupilone-treated cells (IC_{70}). Cytochrome *c* confined in mitochondria was reduced by 66 ± 2% after only 6 h of treatment, and the maximum reduction was achieved at 24 h (83 ± 1%) (Fig. 3B). Cytochrome *c* relocalization was also confirmed by fluorescent microscopy after cell treatment (IC_{70}) for 24 h. Punctuated staining in control cells indicated the presence of cytochrome *c* in intact mitochondria, whereas the diffused fluorescence in treated cells gave evidence of its release in the cytosol (Fig. 3C). Thus, these observations indicate that patupilone induces neuroblastoma cell death by the early disruption of mitochondrial membrane potential followed by cytochrome *c* release.

We showed previously that apoptosis induced by microtubule-stabilizing agents in neuroblastoma cells can be associated with early changes in mitochondria structure (André et al., 2002). Hence, we evaluated patupilone's impact on mitochondria morphology. As shown by electron microscopy (Fig. 4), patupilone (IC_{70}) increased the cristae surface early (6 h), modifying the appearance of mitochondria to a "striped" phenotype. In treated cells, 75 ± 3% of mitochondria were af-

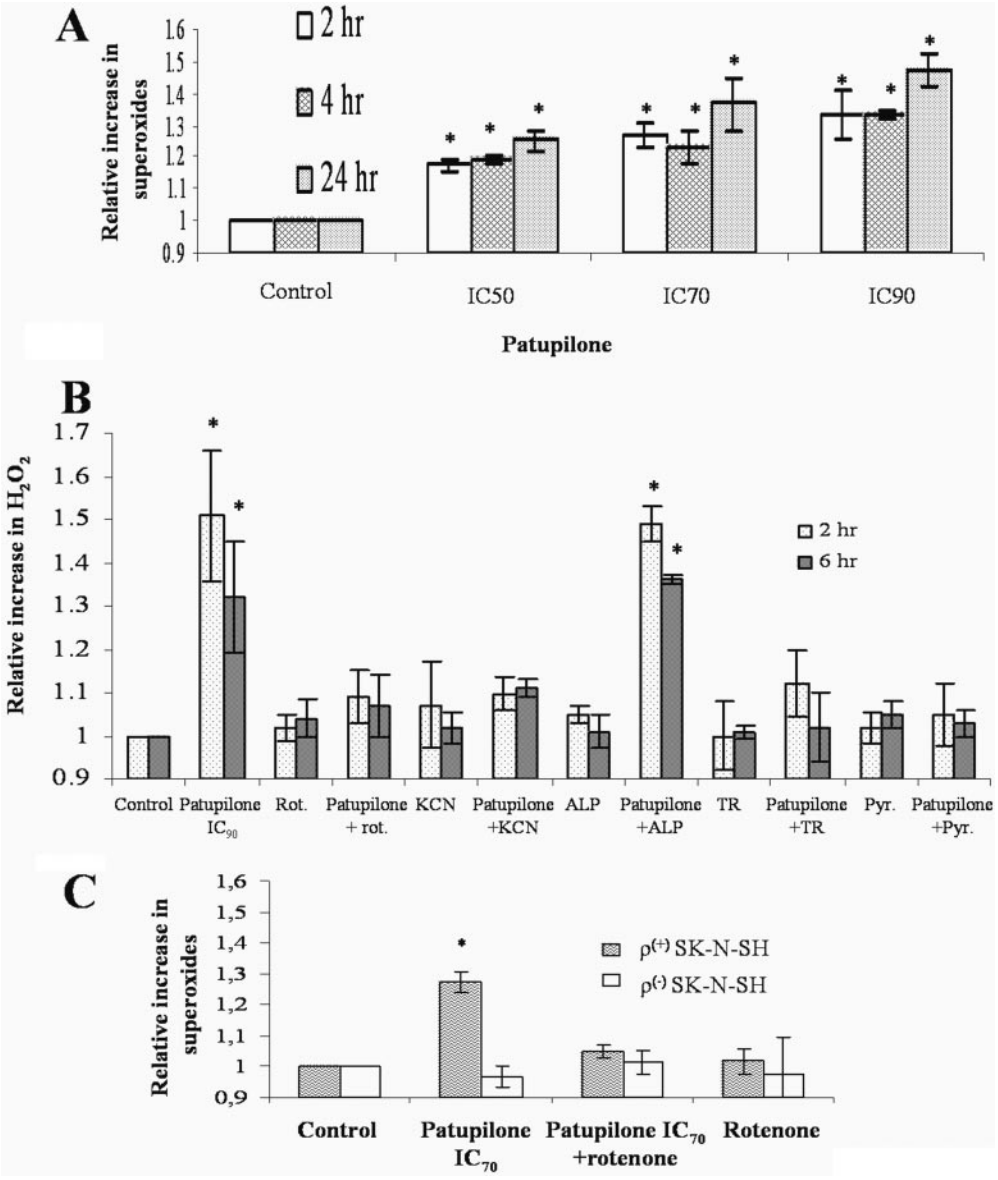

Fig. 5. Patupilone induces ROS production from mitochondria. A, relative production of superoxide ions in SK-N-SH cells during patupilone treatment. B, generation of hydrogen peroxide in SK-N-SH cells incubated with patupilone alone, ROS inhibitors/scavengers alone, or their combinations for 2 or 6 h. Pyr, sodium pyruvate; rot, rotenone; TR, tiron; ALP, allopurinol. C, relative superoxide generation in $\rho^{(+)}$ SK-N-SH and $\rho^{(-)}$ SK-N-SH cells under patupilone (IC_{70}) treatment in the presence or absence of rotenone. Data shown are mean ± S.D. *, $p <$ 0.05 versus control.

fected, whereas it was restricted to a minority in control cells (3 ± 1%).

This change in structure was maintained after a 20-h treatment with patupilone for 76 ± 4% of mitochondria. The swelling and the subsequent nonspecific rupture of mitochondrial membrane only occurred later, affecting 20 ± 3% of mitochondria at 40 h versus 4% in control cells. Altogether, these results show that patupilone affects the mitochondrial membrane integrity early, inducing both morphological and permeability changes.

Increase in Reactive Oxygen Species Specifically Generated by Mitochondria Mediates Patupilone Cytotoxicity. In addition to the established role of mitochondria as reservoir for proapoptotic factors, the mitochondrial compartment constitutes an important generator of ROS. Then, using the WST-1 assay, we first measured $O_2^{\cdot-}$ levels during patupilone treatment. As shown in Fig. 5A, the drug promoted $O_2^{\cdot-}$ production in a concentration-dependent manner. The kinetic analysis of this production revealed a significant increase within the first 2 h of treatment (33 ± 6% increase for IC_{90}), which was maintained up to 24 h. This early effect of patupilone was confirmed by measuring $O_2^{\cdot-}$ by using the lucigenin assay, with a 69 ± 4% increase ($p < 0.01$) for IC_{50} after only 30 min. In parallel, H_2O_2 levels were detected by the DCF-DA test. As observed for $O_2^{\cdot-}$, patupilone (IC_{90}) rapidly enhanced H_2O_2 formation by 51 ± 3% at 2 h, 32 ± 7% at 6 h (Fig. 5B), and 47 ± 5% at 24 h (data not shown).

To determine whether the ROS produced were of mitochondrial origin, we coincubated cells with patupilone and rotenone or KCN, inhibitors of mitochondrial electron transport chain complexes. It is noteworthy that patupilone-mediated increase in H_2O_2 levels was prevented by both rotenone and KCN (Fig. 5B). Likewise, rotenone inhibited $O_2^{\cdot-}$ production induced by patupilone (Fig. 5C). In contrast, allopurinol that inhibits xanthine oxidase, a cytosolic source for cellular $O_2^{\cdot-}$, did not inhibit the patupilone-induced ROS production (Fig. 5B). Thus, patupilone specifically enhanced ROS generation from mitochondria. Finally, sodium pyruvate (H_2O_2 scavenger) was as potent as tiron ($O_2^{\cdot-}$ scavenger) in inhibiting H_2O_2 increase (Fig. 5B), strongly suggesting that the mitochondrial H_2O_2 resulted from $O_2^{\cdot-}$ dismutation.

To further demonstrate the mitochondrial origin of ROS, we compared ROS production induced by patupilone in wild-type SK-N-SH cells [i.e., $\rho^{(+)}$] and SK-N-SH cells that were partially depleted of mitochondrial DNA [i.e., $\rho^{(-)}$]. $\rho^{(-)}$ cells were characterized by a strong inhibition of the mitochondrial energy production, as indicated by the incapacity to grow in glucose-deprived medium (data not shown). These cells do not express essential components of the mitochondrial respiratory chain, as confirmed by the 76 ± 1% decrease in COX II expression, a mitochondrial DNA-encoded protein (Fig. 6A). In contrast with $\rho^{(+)}$ SK-N-SH cells, patupilone did not trigger $O_2^{\cdot-}$ generation in $\rho^{(-)}$ cells (Fig. 5C), confirming that ROS were specifically produced by mitochondria.

To investigate whether mitochondrial ROS were involved in patupilone efficacy, we measured the cytotoxicity of patupilone in $\rho^{(-)}$ cells. It is interesting that $\rho^{(-)}$ cells were markedly resistant to patupilone compared with $\rho^{(+)}$ cells (Fig. 7A). For example, cell survival at IC_{70} (5 nM) was increased from 27 ± 4% in $\rho^{(+)}$ SK-N-SH cells to 59 ± 6% in $\rho^{(-)}$ cells ($p < 0.05$). Because expression of nuclear DNA-encoded proteins of the apoptotic machinery (cytochrome *c*, Bcl-2, Bim, and Bax) remained intact in $\rho^{(-)}$ cells (Fig. 6B), mitochondrial ROS abrogation was responsible for $\rho^{(-)}$ cell resistance to patupilone. Then, we confirmed these results by using tiron and sodium pyruvate in wild-type SK-N-SH cells. As observed in $\rho^{(-)}$ cells, both antioxidants considerably protected cells against patupilone cytotoxic effects when added from the beginning of treatment (Fig. 7, B and C). In combination with patupilone IC_{70}, tiron increased cell survival from 32 ± 1 to 71 ± 2% ($p < 0.05$). Moreover, the IC_{50} value, which was 2 nM for patupilone alone, strongly increased in the presence of tiron and was even not reached at 10 nM patupilone. Similar results were obtained with pyruvate, which protected cells from patupilone as efficiently as tiron. In sharp contrast, the addition of tiron or sodium pyruvate at 24 h of treatment did not modify patupilone activity (Fig. 7, B and C), indicating that late generation of ROS was not responsible for the drug antitumor effects. Altogether, our data show that neuroblastoma cell death induced by patupilone was mediated by the early generation of $O_2^{\cdot-}$ and the subsequent formation of H_2O_2 from mitochondria.

Bim Translocates Early to Mitochondria during Patupilone-Induced Apoptosis. Bim is a proapoptotic protein of the Bcl-2 family and a cytoskeleton resident protein (Puthalakath et al., 1999; Butt et al., 2006). It thus represents a candidate of choice to be translocated toward mitochondria during patupilone-induced apoptosis. Although Bim expression levels did not significantly change in whole cells (Fig. 8A), it was modified in the mitochondrial compartment

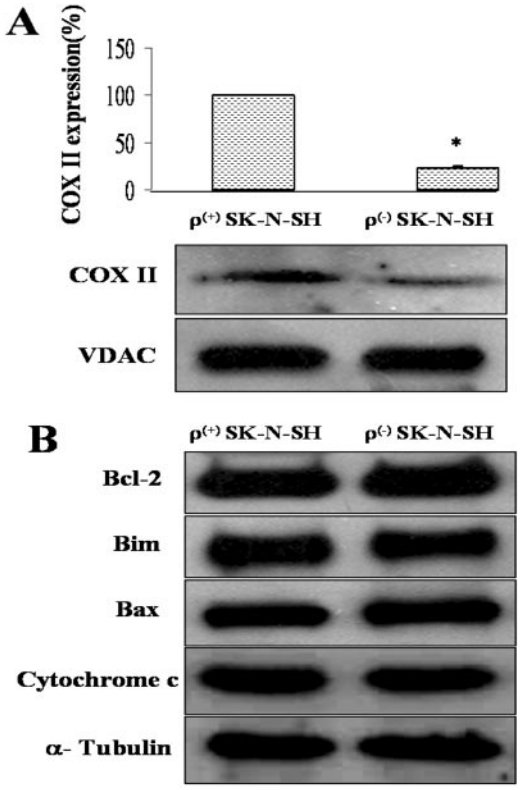

Fig. 6. Decreased expression of COX II in $\rho^{(-)}$ SK-*N*-SH cells. A, Western blot analysis of COX II, voltage-dependent anion channel, and other indicated proteins (B) in whole-cell lysates of $\rho^{(+)}$SK-N-SH cells and derived $\rho^{(-)}$SK-N-SH cells. Histogram is the outcome of protein quantification by software ImageJ and represents mean ± S.D. *, $p < 0.05$ versus control.

(Fig. 8B). Indeed, Bim amount considerably increased (2.4 ± 1.0-fold) in mitochondria isolated from cells treated for only 6 h with patupilone compared with those extracted from control SK-N-SH cells (DMSO-treated) at the same time point. Bim translocation was amplified at 12 h of treatment (3.3 ± 0.7-fold) until a maximum was achieved at 24 h of treatment (4.7 ± 0.7-fold increased) and maintained at 30 h. In parallel, we did not detect any modification in Bak or Bcl-2 expression, and Bcl-2 hyperphosphorylation was only observed for patupilone concentrations that induced mitotic block (data not shown). Thus, regarding Bcl-2 family proteins, Bim accumulation to mitochondria was a specific event induced early by patupilone.

In contrast to Bim, p53 expression was increased by patupilone from 12 h (6.7 ± 0.5 times) in whole SK-N-SH cells (Fig. 8C). Because p53 is also a microtubule-transported protein, we evaluated whether it could be displaced to mitochondria during patupilone-induced apoptosis. We observed that the mitochondria-localized p53 increased during treatment (12.3 ± 1.5 times at 30 h), in contrast with p21 that was completely absent from the mitochondrial fractions (Fig. 8D). However, because accumulation of p53 in mitochondria only started at 12 h, it may amplify mitochondrial permeabilization subsequently to Bim translocation rather than initiate it.

Reactive Oxygen Species Trigger Bim Relocalization and Changes in Mitochondrial Membranes. Because Bim relocalization to mitochondria occurred early in the apoptotic signaling cascade induced by patupilone, we investigated the role of ROS generation in this process. It is interesting that the Bim amount was decreased by 2.3 ± 0.2 and 2.9 ± 0.4 times ($p < 0.05$) in mitochondria isolated from SK-N-SH cells treated with patupilone in the presence of tiron or sodium pyruvate, respectively, compared with patupilone alone (Fig. 9A). Tiron and sodium pyruvate specifically

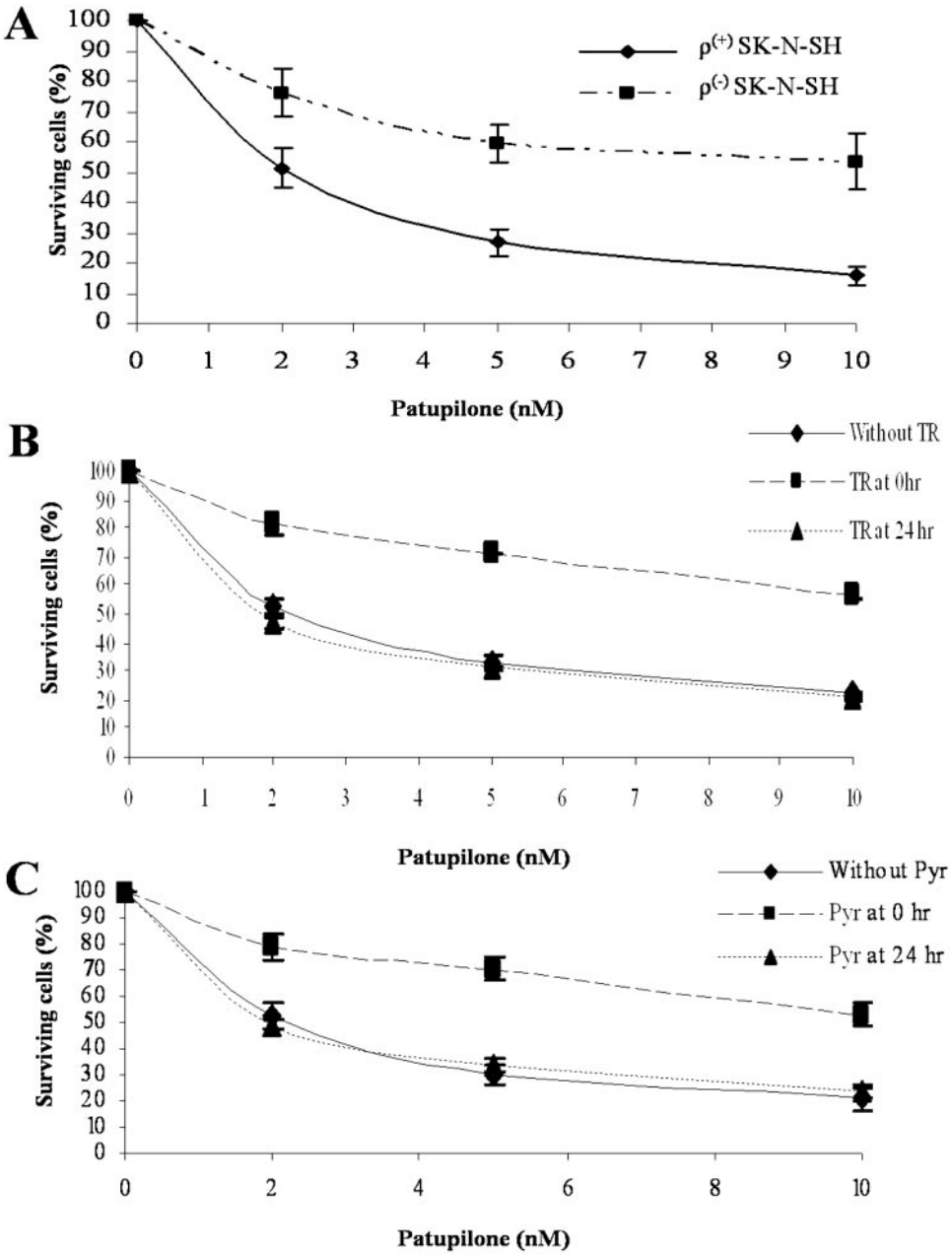

Fig. 7. Mitochondrial ROS participate in patupilone cytotoxicity. A, comparison between $\rho^{(+)}$SK-N-SH and $\rho^{(-)}$SK-N-SH cell sensitivity to patupilone after a 72-h treatment. Concentration-dependent inhibition of SK-N-SH cell survival by patupilone alone after 72-h treatment or combined with tiron (TR; B) and sodium pyruvate (Pyr; C). ROS scavengers were added at indicated time points from the beginning (0 h) and at 24 h during patupilone treatment. Results are expressed as mean ± S.D.

prevented Bim relocalization because no change in Bim expression level was detected in whole cells in the same conditions (data not shown).

Moreover, by inhibiting ROS generation from mitochondria, rotenone also inhibited patupilone-induced Bim translocation (Fig. 9B). The specificity of ROS-governed Bim relocalization was shown by the fact that neither Bcl-2 nor Bax mitochondrial levels were modified during treatment. In parallel, cytochrome *c* release from mitochondria was strongly reduced when patupilone was combined with rotenone (Fig. 9B). By electron microscopy, we showed that the "striped" phenotype of mitochondria induced by patupilone (Fig. 4) was prevented by tiron (Fig. 9C). Altogether, these data indicate that patupilone-mediated production of ROS from mitochondria was responsible for Bim translocation, changes in mitochondrial membrane integrity, and the subsequent neuroblastoma cell death.

Discussion

The role of ROS in apoptotic signaling is the subject of a growing number of studies in cancer cells (Ryter et al., 2007). Increase in ROS production from mitochondria by taxanes is now well established, but ROS contribution to their cytotoxicity is still controversial (Varbiro et al., 2001; André et al., 2002; Park et al., 2004; Fawcett et al., 2005; Patenaude et al., 2007). Moreover, recent reports showed that paclitaxel anticancer activity may also be related to the generation of intracellular and extracellular ROS from the membrane-associated NADPH oxidase (Alexandre et al., 2006, 2007). By using antioxidants and $\rho^{(-)}$ cells, our current study shows that accumulation of mitochondria-derived $O_2^{\cdot-}$ and H_2O_2 is a causal effect of apoptosis induction by patupilone. Furthermore, we determined for the first time that mitochondrial ROS produced early induced Bim relocalization to mitochondria after MTA treatment.

The involvement of mitochondrial ROS in the apoptotic program leads to the question of the events responsible for the increased ROS generation. We showed previously that patupilone directly modified mitochondrial membrane permeability, suggesting that mitochondria may be the target of choice for patupilone to induce apoptosis through ROS production (Khawaja et al., 2006). Several lines of evidence,

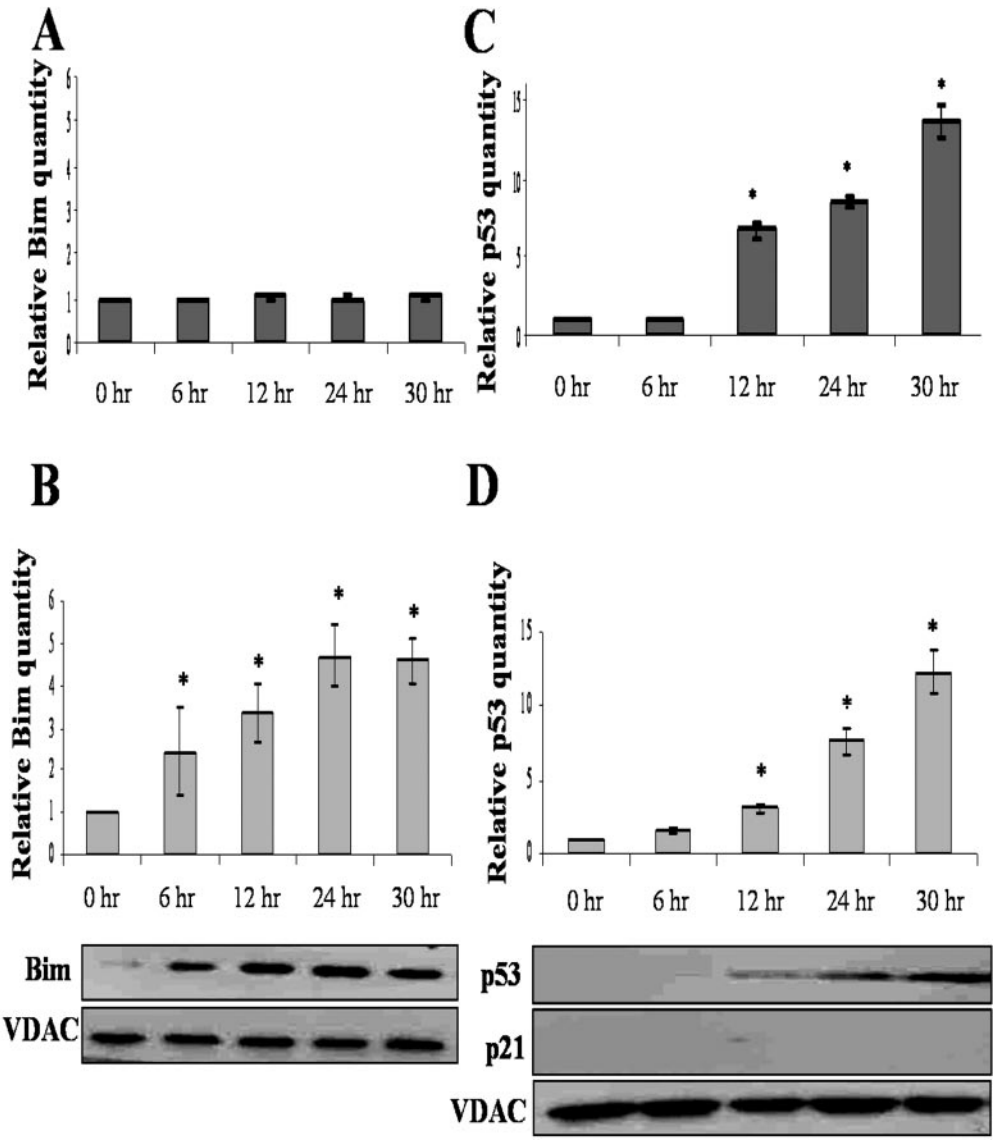

Fig. 8. Patupilone induces Bim and p53 accumulation in mitochondria. Relative quantities of Bim (A) and p53 (C) proteins in whole cells treated with patupilone IC_{70}. Western blot analysis of Bim (B), p53 and p21 (D) variations in mitochondrial fractions. Mitochondria were isolated from SK-N-SH cells after treatment with patupilone IC_{70} or vehicle (up to 30 h). Histograms are the outcome of respective proteins quantification by software ImageJ. Results were expressed as mean ± S.D. *, $p < 0.05$ versus control.

mainly obtained during ceramide-induced apoptosis, indicate that ROS accumulation can be due to an impairment of the mitochondrial respiratory chain (Fleury et al., 2002). Depletion of mitochondrial respiratory chain components in $\rho^{(-)}$ neuroblastoma cells abrogated the increase of ROS levels by patupilone, indicating that patupilone-induced modulation of ROS production may also originate from the dysfunction of the mitochondrial respiratory chain. In agreement with this hypothesis, we showed previously that paclitaxel disturbed the mitochondrial respiration rate in neuroblastoma cells (André et al., 2002). However, it should be noticed that the patupilone IC_{50} value was equally as active in increasing ROS levels as 10 times the IC_{50} value of paclitaxel (i.e., 1 μM,) (André et al., 2002). In addition, we showed previously

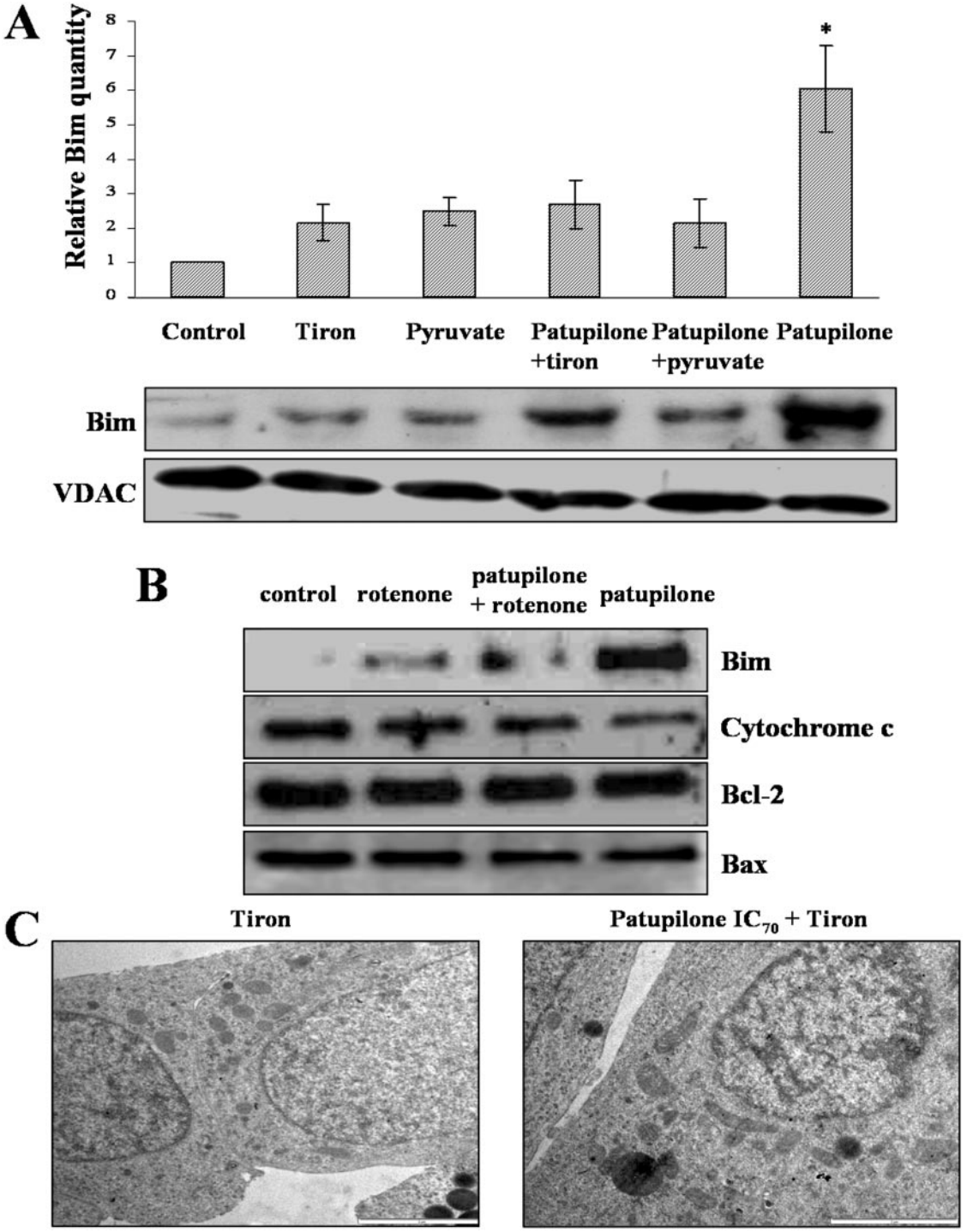

Fig. 9. Mitochondrial ROS trigger Bim relocalization to mitochondria and induce mitochondrial membrane changes. A, Western blot analysis of Bim in mitochondrial fractions. SK-N-SH cells were incubated with patupilone IC_{70} and/or ROS scavengers for 15 h before isolation of mitochondria. The histogram is the outcome of protein quantification by software ImageJ and represents mean ± S.D. *, $p < 0.05$ versus control. B, Western blot directed against Bim, cytochrome *c*, Bcl-2, and Bax in the mitochondrial compartment. Cells were incubated with patupilone IC_{70} and/or rotenone for 6 h before isolation of mitochondria. C, visualization, by transmission electron microscopy, of mitochondria morphology in SK-N-SH cells treated for 12 h with tiron alone or combined with patupilone. Bar, 2 μm.

that patupilone was more efficient than paclitaxel to induce changes in membrane permeability of isolated mitochondria (Khawaja et al., 2006). Altogether, these results may explain a part of the superior activity of patupilone in tumor cells compared with paclitaxel that is, until now, the clinical reference among microtubule-stabilizing agents. Elsewhere, because functions of mitochondria are tightly regulated by their interactions with the microtubule cytoskeleton (Anesti and Scorrano, 2006), patupilone may influence mitochondrial movements, shape, and bioenergetics by modifying microtubule dynamics. Thus, patupilone-mediated ROS production by mitochondria may be related to its ability to strongly stabilize interphasic microtubules during the first 6 h of treatment (Khawaja et al., 2006). Future investigations will determine whether microtubule-directed activity of patupilone is responsible for ROS generation and mitochondrial network disruption.

The molecular link between mitochondrial ROS and MTA activity remains to be established. Here, we showed that the early increase in mitochondrial ROS by patupilone preceded mitochondrial membrane alterations and cytochrome *c* release. A product of $O_2^{\cdot-}$, H_2O_2 displays the ability to directly affect cellular membranes, including mitochondria themselves, by modifying the structure and function of lipids (Petrosillo et al., 2003; Fruehauf and Meyskens, 2007). It is interesting that the lipid peroxidation scavenger trolox did not decrease patupilone activity (personal data), suggesting that mediator(s) might be activated by mitochondrial ROS to trigger, in turn, the loss of mitochondrial membrane integrity.

Mitochondrial membrane permeabilization most generally occurs in response to proapoptotic members of the Bcl-2 family. In contrast to paclitaxel (Tan et al., 2005), patupilone did not increase Bim expression levels to induce apoptosis. Although different models of BH3-only protein interaction with Bax-like and/or Bcl-2-like proteins are discussed currently, it is assumed that Bim-mediated apoptosis requires mitochondrial targeting (Le Bras et al., 2006). However, except for a recent study with the microtubule-depolymerizing agent combretastatin-A4 (Cenciarelli et al., 2008), Bim intracellular distribution has not been evaluated during treatment with MTAs. Our work demonstrates that patupilone triggered Bim accumulation to mitochondria early, which turns the ratio of mitochondria-localized Bcl-2 family proteins in favor of apoptosis. Furthermore, we showed for the first time that Bim accumulation to mitochondria depends on $O_2^{\cdot-}$ and H_2O_2 production by mitochondria themselves. More precisely, we determined that ROS generated in the first 6 h during patupilone-mediated apoptosis were responsible for Bim relocalization. Although H_2O_2 is a relatively weak oxidant, it has emerged as an important signaling molecule mainly based on its capacity to easily diffuse to cellular targets. Because the microtubule network provides the rails for mitochondria trafficking, H_2O_2 may directly affect Bim interaction with microtubules, leading to its translocation to neighboring mitochondria. Elsewhere, Bim activation may also result from its specific phosphorylation by JNK, as described during treatment with a plant toxin (persin), which also acts as a microtubule-stabilizing agent (Butt et al., 2006). In support of this hypothesis, JNK has been shown recently to be activated by ROS during apoptosis (Feng et al., 2007). However, we did not measure an increase in active JNK, and patupilone cytotoxicity was not changed by the specific inhibition of JNK (N. R. Khawaja, D. Braguer, unpublished observations). These data strongly suggest that JNK is not the kinase responsible for Bim activation and translocation to mitochondria during patupilone-induced apoptosis. Future investigations will determine whether other kinases, such as p38 mitogen-activated protein kinase, could be activated by ROS and phosphorylate Bim. Whatever the event responsible for its release, Bim seems to be a molecular mediator to bridge the effects of patupilone on both microtubules and mitochondria.

New insights into apoptotic pathways are urgently needed to promote the development of rationally targeted cancer therapeutics. The role of ROS in cancer cell response to drugs is emerging as an important area of exploration. Altogether, our data identified ROS generation from mitochondria as a central event mediating apoptosis induced by patupilone. They also suggest a key communication between microtubules, which govern intracellular transport, and the mitochondria compartment, which plays simultaneously the role of activator and integrator of apoptotic signals.

References

Adams JM and Cory S (2007) The Bcl-2 apoptotic switch in cancer development and therapy. *Oncogene* **26:**1324–1337.

Alexandre J, Batteux F, Nicco C, Chéreau C, Laurent A, Guillevin L, Weill B, and Goldwasser F (2006) Accumulation of hydrogen peroxide is an early and crucial step for paclitaxel-induced cancer cell death both in vitro and in vivo. *Int J Cancer* **119:**41–48.

Alexandre J, Hu Y, Lu W, Pelicano H, and Huang P (2007) Novel action of paclitaxel against cancer cells: bystander effect mediated by reactive oxygen species. *Cancer Res* **67:**3512–3517.

Altmann KH, Pfeiffer B, Arseniyadis S, Pratt BA, and Nicolaou KC (2007) The chemistry and biology of epothilones-the wheel keeps turning. *Chem Med Chem* **2:**396–423.

André N, Carré M, Brasseur G, Pourroy B, Kovacic H, Briand C, and Braguer D (2002) Paclitaxel targets mitochondria upstream of caspase activation in intact human neuroblastoma cells. *FEBS Lett* **532:**256–260.

André N, Braguer D, Brasseur G, Gonçalves A, Lemesle-Meunier D, Guise S, Jordan MA, and Briand C (2000) Paclitaxel induces release of cytochrome *c* from mitochondria isolated from human neuroblastoma cells. *Cancer Res* **60:**5349–5353.

Anesti V and Scorrano L (2006) The relationship between mitochondrial shape and function and the cytoskeleton. *Biochim Biophys Acta* **1757:**692–699.

Archer SL, Gomberg-Maitland M, Maitland ML, Rich S, Garcia JG, and Weir EK (2008) Mitochondrial metabolism, redox signaling, and fusion: a mitochondria-ROS-HIF-1alpha-Kv1.5 O2-sensing pathway at the intersection of pulmonary hypertension and cancer. *Am J Physiol Heart Circ Physiol* **294:**H570–H578.

Bollag DM, McQueney PA, Zhu J, Hensens O, Koupal L, Liesch J, Goetz M, Lazarides E, and Woods CM (1995) Epothilones, a new class of microtubule-stabilizing agents with a Taxol-like mechanism of action. *Cancer Res* **55:**2325–2333.

Butt AJ, Roberts CG, Seawright AA, Oelrichs PB, Macleod JK, Liaw TY, Kavallaris M, Somers-Edgar TJ, Lehrbach GM, Watts CK, et al. (2006) A novel plant toxin, persin, with in vivo activity in the mammary gland, induces Bim-dependent apoptosis in human breast cancer cells. *Mol Cancer Ther* **5:**2300–2309.

Cenciarelli C, Tanzarella C, Vitale I, Pisano C, Crateri P, Meschini S, Arancia G, and Antoccia A (2008) The tubulin-depolymerising agent combretastatin-4 induces ectopic aster assembly and mitotic catastrophe in lung cancer cells H460. *Apoptosis* **13:**659–669.

Estève MA, Carré M, Bourgarel-Rey V, Kruczynski A, Raspaglio G, Ferlini C, and Braguer D (2006) Bcl-2 down-regulation and tubulin subtype composition are involved in resistance of ovarian cancer cells to vinflunine. *Mol Cancer Ther* **5:**2824–2833.

Estève MA, Carré M, and Braguer D (2007) Microtubules in apoptosis induction: are they necessary? *Curr Cancer Drug Targets* **7:**713–729.

Fawcett H, Mader JS, Robichaud M, Giacomantonio C, and Hoskin DW (2005) Contribution of reactive oxygen species and caspase-3 to apoptosis and attenuated ICAM-1 expression by paclitaxel-treated MDA-MB-435 breast carcinoma cells. *Int J Oncol* **27:**1717–1726.

Feng R, Ni HM, Wang SY, Tourkova IL, Shurin MR, Harada H, and Yin XM (2007) Cyanidin-3-rutinoside, a natural polyphenol antioxidant, selectively kills leukemic cells by induction of oxidative stress. *J Biol Chem* **282:**13468–13476.

Ferlini C, Raspaglio G, Mozzetti S, Distefano M, Filippetti F, Martinelli E, Ferrandina G, Gallo D, Ranelletti FO, and Scambia G (2003) Bcl-2 down-regulation is a novel mechanism of paclitaxel resistance. *Mol Pharmacol* **64:**51–58.

Fleury C, Mignotte B, and Vayssière JL (2002) Mitochondrial reactive oxygen species in cell death signaling. *Biochimie* **84:**131–141.

Fruehauf JP and Meyskens FL Jr (2007) Reactive oxygen species: a breath of life or death? *Clin Cancer Res* **13:**789–794.

Honoré S, Kovacic H, Pichard V, Briand C, and Rognoni JB (2003) $\alpha 2\beta 1$-Integrin signaling by itself controls G_1/S transition in a human adenocarcinoma cell line

(Caco-2): implication of NADPH oxidase-dependent production of ROS. *Exp Cell Res* **285:**59–71.
Jordan MA and Kamath K (2007) How do microtubule-targeted drugs work? An overview. *Curr Cancer Drug Targets* **7:**730–742.
Khawaja NR, Carre M, Pourroy B, Kovacic H, and Braguer D (2006) High potency of epothilones in neuroblastoma cells may involve mitochondria. In: Proceedings of 96th Annual Meeting of American Association of Cancer Research; 2005 Apr 16–20; Anaheim, CA. Philadelphia, PA, American Association of Cancer Research, p. 118, abstract 498.
Le Bras M, Rouy I, and Brenner C (2006) The modulation of inter-organelle cross-talk to control apoptosis. *Med Chem* **2:**1–12.
Lee FY, Smykla R, Johnston K, Menard K, McGlinchey K, Peterson RW, Wiebesiek A, Vite G, Fairchild CR, and Kramer R (2008) Preclinical efficacy spectrum and pharmacokinetics of ixabepilone. *Cancer Chemother Pharmacol,* in press.
Li R, Moudgil T, Ross HJ, and Hu HM (2005) Apoptosis of non-small-cell lung cancer cell lines after paclitaxel treatment involves the BH3-only proapoptotic protein Bim. *Cell Death Differ* **12:**292–303.
Li Z, Zhang J, Liu Z, Woo CW, and Thiele CJ (2007) Downregulation of Bim by brain-derived neurotrophic factor activation of TrkB protects neuroblastoma cells from paclitaxel but not etoposide or cisplatin-induced cell death. *Cell Death Differ* **14:**318–326.
Morazzani M, de Carvalho DD, Kovacic H, Smida-Rezgui S, Briand C, and Penel C (2004) Monolayer versus aggregate balance in survival process for EGF-induced apoptosis in A431 carcinoma cells: Implication of ROS-P38 MAPK-integrin alpha2beta1 pathway. *Int J Cancer* **110:**788–799.
Nettles JH, Li H, Cornett B, Krahn JM, Snyder JP, and Downing KH (2004) Downing KH. The binding mode of epothilone A on alpha, beta-tubulin by electron crystallography. *Science* **305:**866–869.
Newmeyer DD and Ferguson-Miller S (2003) Mitochondria: releasing power for life and unleashing the machineries of death. *Cell* **112:**481–490.
Nicolaou KC, Winssinger N, Pastor J, Ninkovic S, Sarabia F, He Y, Vourloumis D, Yang Z, Li T, Giannakakou P, et al. (1997) Synthesis of epothilones A and B in solid and solution phase. *Nature* **387:**268–272.
Orr GA, Verdier-Pinard P, McDaid H, and Horwitz SB (2003) Mechanisms of Taxol resistance related to microtubules. *Oncogene* **22:**7280–7295.
Park SJ, Wu CH, Gordon JD, Zhong X, Emami A, and Safa AR (2004) Taxol induces caspase-10-dependent apoptosis. *J Biol Chem* **279:**51057–51067.
Pasquier E, Honoré S, and Braguer D (2006) Microtubule-targeting agents in angiogenesis: where do we stand? *Drug Resist Update* **9:**74–86.
Patenaude A, Deschesnes RG, Rousseau JL, Petitclerc E, Lacroix J, Côté MF, and C-Gaudreault R (2007) New soft alkylating agents with enhanced cytotoxicity against cancer cells resistant to chemotherapeutics and hypoxia. *Cancer Res* **67:**2306–2316.
Petrosillo G, Ruggiero FM, and Paradies G (2003) Role of reactive oxygen species and cardiolipin in the release of cytochrome c from mitochondria. *FASEB J* **17:**2202–2208.
Pourroy B, Carré M, Honoré S, Bourgarel-Rey V, Kruczynski A, Briand C, and Braguer D (2004) Low concentrations of vinflunine induce apoptosis in human SK-N-SH neuroblastoma cells through a postmitotic G_1 arrest and a mitochondrial pathway. *Mol Pharmacol* **66:**580–591.
Putcha GV, Moulder KL, Golden JP, Bouillet P, Adams JA, Strasser A, and Johnson EM (2001) Induction of BIM, a proapoptotic BH3-only BCL-2 family member, is critical for neuronal apoptosis. *Neuron* **29:**615–628.
Puthalakath H, Huang DC, O'Reilly LA, King SM, and Strasser A (1999) The proapoptotic activity of the Bcl-2 family member Bim is regulated by interaction with the dynein motor complex. *Mol Cell* **3:**287–296.
Ryter SW, Kim HP, Hoetzel A, Park JW, Nakahira K, Wang X, and Choi AM (2007) Mechanisms of cell death in oxidative stress. *Antioxid Redox Signal* **9:**49–89.
Sève P, Reiman T, Lai R, Hanson J, Santos C, Johnson L, Dabbagh L, Sawyer M, Dumontet C, and Mackey JR (2007) Class III beta-tubulin is a marker of paclitaxel resistance in carcinomas of unknown primary site. *Cancer Chemother Pharmacol* **60:**27–34.
Tan TT, Degenhardt K, Nelson DA, Beaudoin B, Nieves-Neira W, Bouillet P, Villunger A, Adams JM, and White E (2005) Key roles of BIM-driven apoptosis in epithelial tumors and rational chemotherapy. *Cancer Cell* **7:**227–238.
Taniguchi T, Takahashi M, Shinohara F, Sato T, Echigo S, and Rikiishi H (2005) Involvement of NF-kappaB and mitochondrial pathways in docetaxel-induced apoptosis of human oral squamous cell carcinoma. *Int J Mol Med* **15:**667–673.
Varbiro G, Veres B, Gallyas F Jr, and Sumegi B (2001) Direct effect of Taxol on free radical formation and mitochondrial permeability transition. *Free Radic Biol Med* **31:**548–558.

Address correspondence to: Dr. Diane Braguer, INSERM UMR911, Faculté de Pharmacie, 27 Bd Jean Moulin, 13385 Marseille Cedex 05, France. E-mail: diane.braguer@univmed.fr